Available online at www.sciencedirect.com
SCIENCE DIRECT®

Diamond & Related Materials 15 (2006) 1117 – 1121

DIAMOND AND RELATED MATERIALS
www.elsevier.com/locate/diamond

Investigations of heavy ion irradiation of gallium nitride nanowires and nanocircuits

V.M. Ayres [a,*], B.W. Jacobs [a], M.E. Englund [a], E.H. Carey [a], M.A. Crimp [a], R.M. Ronningen [a], A.F. Zeller [a], J.B. Halpern [b], M.-Q. He [b], G.L. Harris [b], D. Liu [c], H.C. Shaw [d], M.P. Petkov [e]

[a] *Department of Electrical and Computer Engineering, Michigan State University, East Lansing, MI 48824, USA*
[b] *Howard University, Washington, DC 20059, USA*
[c] *Muniz Engineering Inc., Greenbelt, MD 20771, USA*
[d] *NASA Goddard Space Flight Center, Greenbelt, MD 20771, USA*
[e] *NASA Jet Propulsion Laboratory, Pasadena, CA 91109, USA*

Available online 7 February 2006

Abstract

Results of a first investigation of the response of gallium nitride nanowires to high-Z heavy ion irradiation are reported. Pre-irradiation characterization of the gallium nitride nanowires used in these experiments showed that that they had a two-phase coaxial structure, consisting of an outer shell of zinc–blende-phase gallium nitride and a coaxial core of wurtzite-phase gallium nitride. Observed radiation interactions with the two-phase structure are reported. A nanowire-based field effect transistor using these GaN nanowires showed normal real-time operation during irradiation by Krypton-78 heavy ions under high bias conditions.

Keywords: Gallium nitride (GaN); Radiation-induced effects; High-resolution electron microscopy; Nanotechnology

1. Introduction

Experimental results indicate that across the main radiation environments, including heavy ion [1], total ionizing dose [2] and proton irradiation [3], different types of nanoscale materials and circuits may outperform their conventional counterparts. In each reported case, the improvement was traced to the use of a nanoscale functional entity and its apparent radiation resiliency.

We will present investigations of the response of gallium nitride (GaN) nanowires and nanocircuits to heavy ion radiation that simulates space radiation environments. The heavy ion radiation experiments were performed at the National Superconducting Cyclotron Laboratory at Michigan State University, whose available beam energies well match the energy spectra of abundant charged particles in space radiation environments. In these experiments the GaN nanowires and nanocircuits were irradiated using a primary beam of ^{78}Kr at 140.32 MeV per nucleon (MeV/u), delivered by the coupled cyclotron facility at the National Superconducting Cyclotron Laboratory (NSCL), with beam parameters as described in Reference [4]. The experiments were performed in the NSCL S1 Vault Single Event Excitation Test Facility (SEETF), which is specially equipped with electronic and beam operations connections to a remote control room [5]. This enabled the first real-time characterization of the electronic performance of a GaN-based field effect transistor (FET) during ^{78}Kr irradiation. Irradiations of GaN nanowires were also carried out separately under the same beam conditions.

We will present the results of three sets of experiments: (1) a summary of the real-time electronic performance of the GaN nanowire FET during ^{78}Kr irradiation; (2) a summary of the pre-radiation structural characterization of the GaN nanowires; and (3) a first post radiation structural characterization of the GaN nanowires after ^{78}Kr irradiation.

2. Experimental results

2.1. Summary of real-time electronic performance of irradiated GaN nanocircuits

We will summarize real-time GaN nanocircuit performance during irradiation previously reported in References [4] to show

* Corresponding author. Tel.: +1 517 355 5236; fax: +1 517 353 1980.
E-mail address: ayresv@egr.msu.edu (V.M. Ayres).

0925-9635/$ - see front matter © 2006 Elsevier B.V. All rights reserved.
doi:10.1016/j.diamond.2005.11.055

the potential that nanowire based devices may have in radiation environments. A GaN nanowire FET design using the nanowire as an *n*-type semiconducting channel [6] was used in the radiation experiments. The nanowire was connected to contacts pads using electron beam lithography and wire-bonded to a dual-in-line package, as shown in Fig. 1(a–b). Nanotube/nanowire FET designs achieve transistor functionality via unconventional Schottky barrier modulation at the contacts rather than by standard channel modulation [7,8], as shown in Fig. 2. The *I–V* characteristics of the FET were taken before, during and after irradiation with different gate-source voltages (V_{GS}) and swept source-drain voltages (V_{SD}), using a Keithley 487 Picoammeter/Voltage Source and a Hewlett-Packard 6633A System DC Power Supply. Measured pre-radiation *I–V* characteristics at V_{GS} of 0, 3, and 6 V demonstrated that the nanowire was *n*-type and its conduction could be altered by varying V_{GS}.

Real-time electronic measurements during ^{78}Kr heavy ion irradiation were implemented in LabVIEW [9] using a remote-connection computer during the experiments. All measurements were made in air at room temperature. Irradiation was initiated at a low level intensity of 10^2 particles per second (pps), and subsequently increased to 10^6 pps with intermediate intensities of 10^4 pps and 10^5 pps. The gate voltage was also increased through 0, 3, 6, and 9 V. Each combination of conditions was maintained for 600 s; therefore, the beam fluence per run ranged from 3×10^4 to 3×10^7 particles/cm^2. The selected radiation levels corresponded to the ones that have caused electronic upsets in conventional circuits during ^{78}Kr irradiation [10] and were the highest available at the SEETF facility.

The real-time *I–V* characteristics of the active GaN nanowire FET during ^{78}Kr irradiation are shown in Fig. 3. The final active nanocircuit conditions were $V_{GS}=9$ V and $V_{SD}=0$–22 V, under 5×10^5 particles/sec/cm^2. The results indicated normal real-time electronic function. At the conclusion of the radiation experiments, after exposure to a cumulative fluence of 3.30×10^7 particles/cm^2, the post-radiation electronic performance of the GaN FET was again measured, first at V_{GS} of 9 V followed by V_{GS} of 12 V. Normal electronic function was observed under these post-irradiation high bias conditions.

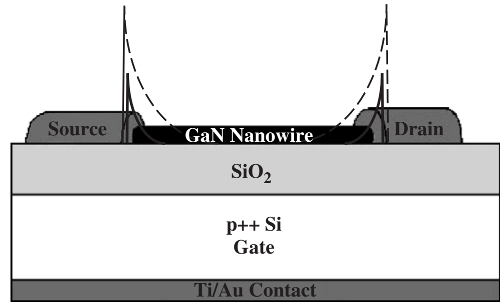

Fig. 2. Nanowire field effect transistor design. A gate bias is used to thin and lower (solid) or thicken and raise (dashed) the contact-nanowire Schottky barrier via a field effect across the oxide layer.

2.2. Summary of pre-irradiation characterization of GaN nanowires

The stable performance of the GaN FET nanocircuit is determined by both the nanowire properties and the nanocircuit architecture. In this paper, we are presenting the results of the first investigation of the GaN nanowire response to high-Z heavy ions interactions. In order to understand the post-irradiation results, a summary of the pre-irradiation characterization of the GaN nanowires is presented next.

The GaN nanowires were grown in a direct reaction of metal gallium vapor with flowing ammonia at 850–900 °C without a catalyst, resulting in diameters of ~50–100 nm [11,12]. Our group has analyzed over thirty GaN nanowires grown under these conditions using a JEOL FS2200 high-resolution transmission electron microscope (HRTEM). A typical HRTEM image is shown in Fig. 4(a). An approximately 5 nm surface oxide layer is followed by a 20–60 nm outer layer and a 30–40 nm coaxial inner core. Fast Fourier Transforms (FFTs) shown in Fig. 4(b) indicate that the outer shell is zinc–blende-phase gallium nitride and that the coaxial core is wurtzite-phase gallium nitride. Nanodiffraction, selected area diffraction, energy-dispersive spectroscopy and electron energy loss spectroscopy results were consistent with the FFT results. The inner core and the outer layer are both highly crystalline with a sharp ~2–3 atomic layer interface. All the GaN nanowires

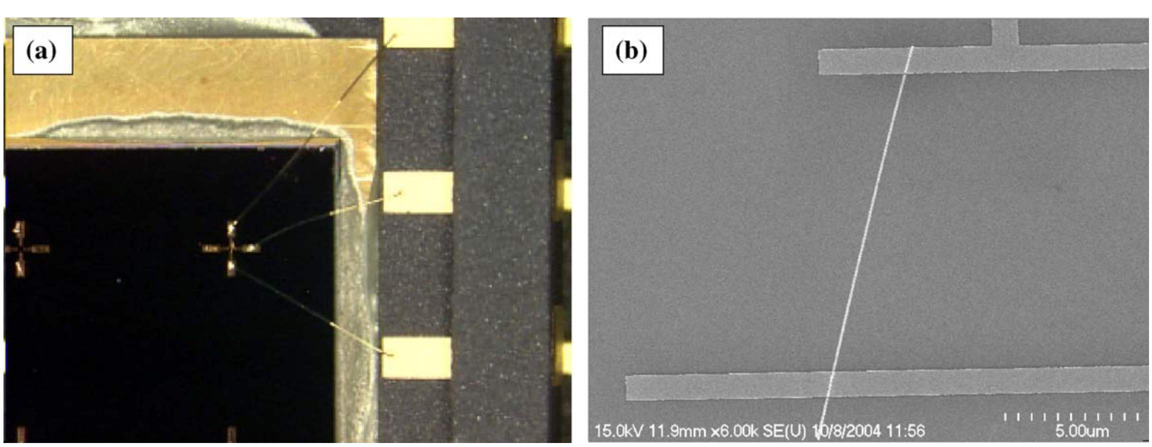

Fig. 1. (a) Wire-bonding of dual-in-line package to the large contact pads. The large contact pads are also connected to the nanowire by electron beam lithographically fabricated leads. (b) SEM image of a top view of the GaN nanowire and electron beam lithographically leads, on the oxide layer.

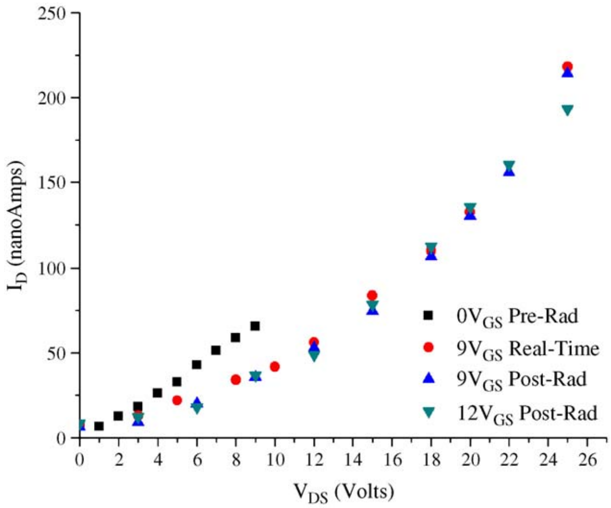

Fig. 3. The GaN nanowire FET *I–V* characteristics for: pre-irradiation with 0 V bias; real-time irradiation, with 9 V bias; post-irradiation with 9 V bias; and post-irradiation with 12 V bias.

analyzed by our group to date have shown this coaxial structure, when fabricated as described in References [11,12].

2.3. Post-irradiation characterization of GaN nanowires

In the nanomaterials experiments, a volume of material was prepared and weighed using a Denver Instruments M-220D with 0.01 mg place accuracy prior to the experiments. The measured sample mass of the GaN nanowires plus amorphous GaN matrix (shown in Fig. 5(a)) was 0.0374 g. The GaN sample was mounted behind a thin ~0.25 mm mica sheet on a *p*-type silicon substrate (with native oxide) as shown in Fig. 5(b). The SEETF beam path passed through a 0.075 mm zirconium foil vacuum exit window, a 0.27 mm four-quadrant plastic scintillator plate used to continuously monitor the incoming ^{78}Kr beam current, a 432 mm air gap, and the 0.25 mm mica restraining sheet. Beam energy calculations performed using the stopping range of ions in matter (SRIM) [13]. Monte Carlo code indicated losses of 2.9, 2.7, 4.6 and 5.4 MeV/u, in the zirconium foil vacuum exit window, the four-quadrant plastic scintillator plate, the air gap, and the mica restraining sheet. This resulted in an on-target beam energy of 124.8 MeV/u. The GaN nanomaterial sample was exposed to a uniform 1×2 cm^2 beam centered on the ~0.16 cm^2 sample by laser alignment. The highest radiation dose was 6.4×10^5 particles per second (pps) ^{78}Kr irradiation, for 900 s. This resulted in cumulative energy deposition in the GaN sample of ~355 Gray (1 Gy = 1 J/kg).

Seven individual GaN nanowires have been examined to date using HRTEM. Five have shown no visible signs of damage, and their appearance and diffraction patterns are similar to those shown in Fig. 4. Two GaN nanowires have shown evidence of radiation damage. A wide area TEM image of the radiation damage observed in one GaN nanowire is shown in Fig. 6(a). The single-line and double-line boxes indicate the outer layer and interface/core areas investigated with HRTEM and Fast Fourier Transforms (FFTs). A transformation to amorphous material by the outer layer area is indicated by the Fast Fourier Transform (inset) with a concentric ring pattern shown in Fig. 6(b) and by the general appearance of the phase contrast image. However, the FFT also shows spots from the remaining zinc–blende (ZB) crystalline structure. The ZB crystalline diffraction pattern is on or close to the (011) zone axis. An HRTEM with FFTs of both the core (left inset) and interface (right inset) areas is shown in Fig. 6(c). The left inset Fast Fourier Transform of the core area indicates a wurtzite crystalline structure with a zone axis close to the 001 axis (the *c*-axis). The right inset Fast Fourier Transform of the interface area indicates a crystalline zinc–blende structure close to the (011) zone axis. This corresponds with the crystal structure and orientation of the outer layer shown in Fig. 6(b), but without the strong concentric rings.

Fig. 7 shows a second GaN nanowire with evidence of radiation damage. Plumes (dashed line box) were observed along the upper side of the nanowire while gouges (black solid line box) were observed along the bottom side, as shown in Fig. 7(a). Fast Fourier Transforms of the core area (double-line box, Fig. 7(a)) indicated an undamaged wurtzite crystalline structure. Fast Fourier Transforms along the gouged side, indicated a ZB crystalline structure with faint amorphous rings. This pattern was observed both on (black line box) and off (white line box)

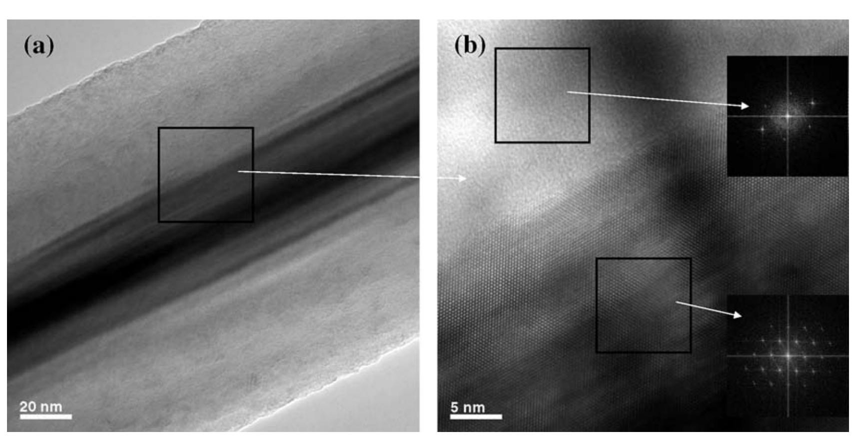

Fig. 4. (a) TEM image of GaN nanowire shows typical inner core and a coaxial outer layer. The box indicates the close-up area in (b) HRTEM image with Fast Fourier Transforms (insets) indicate that the outer shell is zinc–blende phase gallium nitride and that the coaxial core is wurtzite-phase gallium nitride.

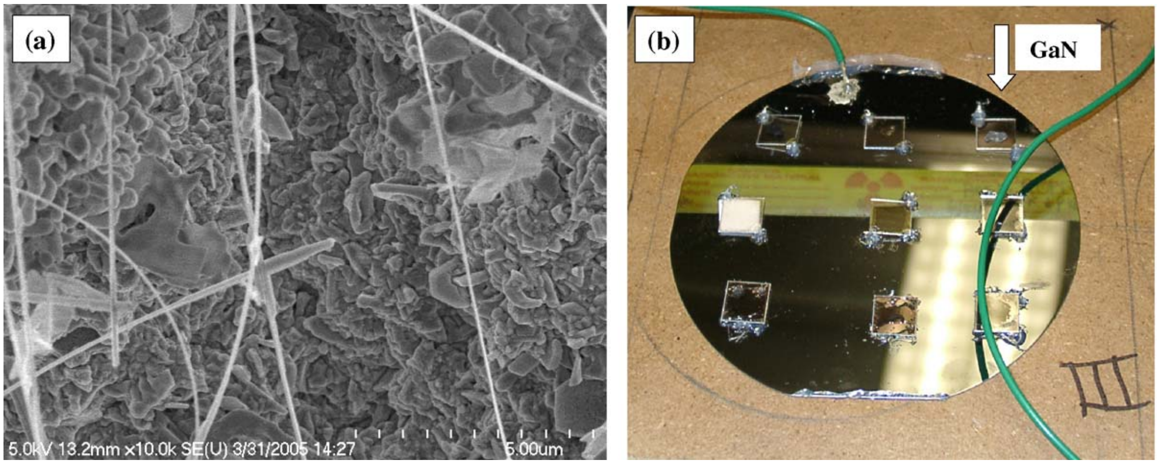

Fig. 5. (a) SEM image of the GaN nanomaterial sample showing GaN nanowires in a GaN matrix. (b) Experimental configuration for the nanomaterials experiments. A GaN nanomaterial sample is indicated by the arrow.

the gouged sites. By contrast, strong concentric rings indicating amorphous material were observed in Fast Fourier Transforms for all areas along the plumed side, as shown in Fig. 7(b).

3. Discussion

A GaN nanowire-based field effect transistor circuit has shown normal real-time operation during irradiation by ^{78}Kr heavy ions, under high bias conditions. Normal post-irradiation electronic behavior under high bias conditions was also observed. These results demonstrate the potential that nanowire-based devices may have to function well in radiation environments.

The stable performance of the GaN FET nanocircuit is determined by both the nanowire properties and the nanocircuit architecture. In this paper, we have presented the results of the first investigation of the GaN nanowire properties with their response to high-Z heavy ions interactions. Pre-irradiation characterization of the GaN nanowires used in these experiments by HRTEM, nanodiffraction, SAD, EDS and EEELS has shown that that these GaN nanowires had a two-phase coaxial structure: an outer shell of zinc–blende-phase gallium nitride and a coaxial core of wurtzite-phase gallium nitride.

The observed radiation response of the two-phase coaxial GaN nanowire structure may be summarized as follows. The

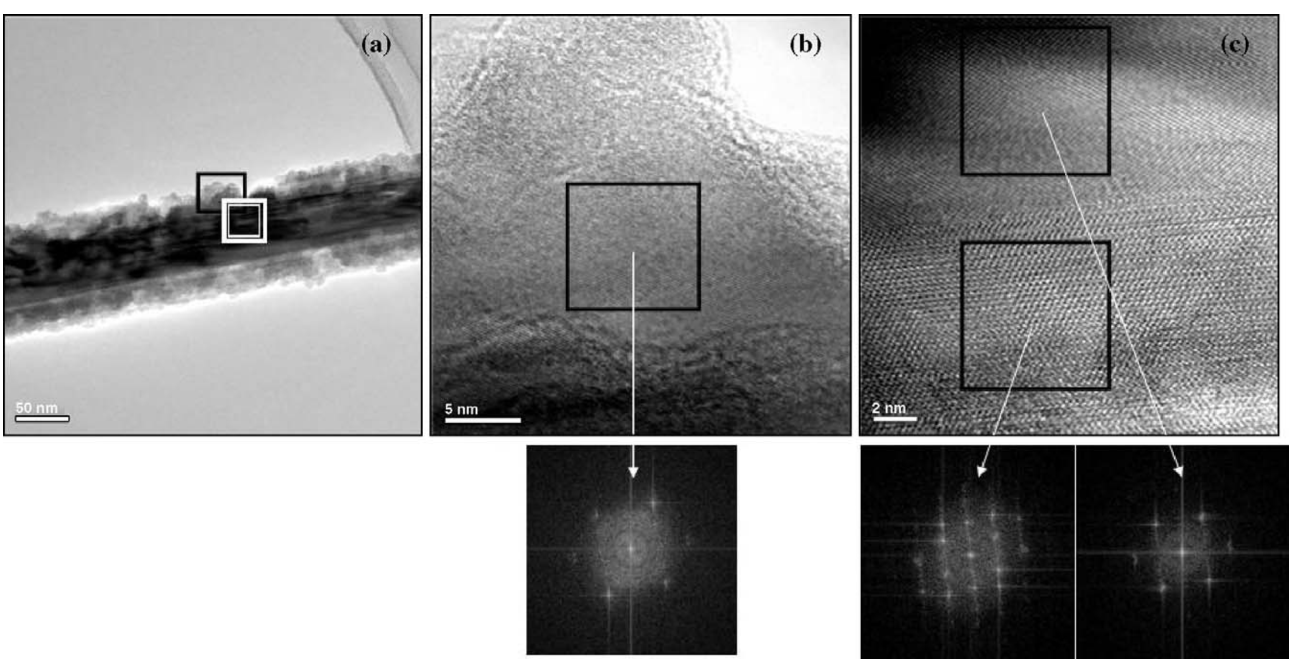

Fig. 6. (a) Wide area TEM image of the radiation damage observed in a GaN nanowire. The blue and red boxes indicate the areas investigated in (b) and (c). (b) A transformation to amorphous material is indicated by the Fast Fourier Transform (inset) with a strong concentric ring pattern although crystalline zinc–blende diffraction sport are still observed. (c) HRTEM of both interface and core areas. The left inset Fast Fourier Transform of the core indicates a wurtzite crystalline structure. The right inset Fast Fourier Transform of the interface indicates a crystalline zinc–blende structure with a faint amorphous ring.

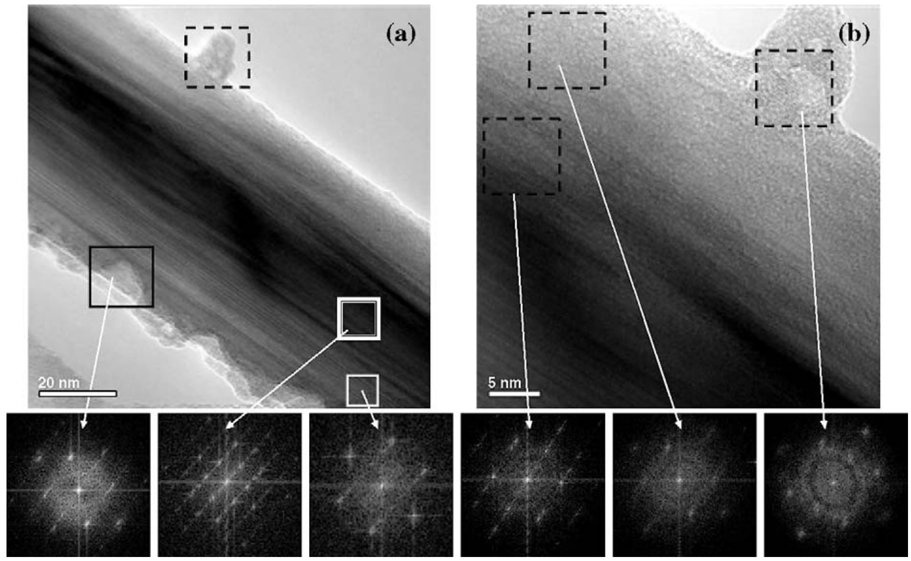

Fig. 7. (a) Wide area TEM image of plume (red box) and gouge (yellow box) observed in a second irradiated GaN nanowire. Fast Fourier Transforms along the core (blue box) indicate an undamaged wurtzite crystalline structure. Fast Fourier Transforms along the gouged side show faint amorphous rings. (b) Strong amorphous rings are observed in Fast Fourier Transforms of areas along the plumed side.

majority of the GaN nanowires examined to date did not show strong evidence of radiation coupling; however, these investigations are continuing. Two GaN nanowires did shown evidence of radiation damage. The heavy ion interaction could result in the creation of plumes of amorphous material along the coaxial zinc–blende outer layer. The GaN wurtzite core did not show evidence of substantial departure from crystallinity. No propagation or accumulation of defects at the zinc–blende/wurtzite interface has been observed to date.

Two imperfect structures along the irradiated GaN surfaces have been observed, which are referred to as plumes and gouges. All plumes investigated to date have shown strong concentric ring patterns indicating amorphous material in corresponding FFTs. This was also true for outer layers adjacent to the plumes. However, FFTs of the gouges and their adjacent areas have indicated largely crystalline material. Gouges have sometimes also been observed in non-irradiated GaN nanowires. This suggests that heavy ion radiation may be coupled to previously damaged GaN nanowires via defect sites. A set of deliberately damaged GaN nanowires will be investigated in future heavy ion irradiation experiments to test this hypothesis.

Acknowledgements

The authors thank the NSCL operations staff for providing the ^{78}Kr beam and their technical support. This research was supported by the National Aeronautic and Space Administration under NASA GSFC Task No. 14 and by the National Science Foundation under Grant No. PHY-0110253.

References

[1] B.W. Jacobs, V.M. Ayres, M.A. Crimp, R.M. Ronningen, A.F. Zeller, H.C. Shaw, A.J. Kogut, J.B. Benavides, M.P. Petkov, J.B. Halpern, in: Mircea Chipara, David L. Edwards, Roberto S. Benson, Shawn Phillips (Eds.), Materials for Space Applications, Mater. Res. Soc. Symp. Proc., vol. 851, Warrendale, PA, 2005, p. 287.

[2] M.P. Petkov, L.D. Bell, H.A. Atwater, IEEE Trans. Nucl. Sci. 51 (2004) 3822.

[3] R. Leon, S. Marcinkevicius, J. Siegert, B. Cechavicius, B. Magness, W. Taylor, C. Lobo, IEEE Trans. Nucl. Sci. 49 (2002) 2844.

[4] V.M. Ayres, B.W. Jacobs, S.P. Song, R.M. Ronningen, A.F. Zeller, M.A. Crimp, J.B. Halpern, M.-.Q. He, M.P. Petkov, D. Liu, H.C. Shaw, in: Edward W. Taylor (Ed.), Proceedings of SPIE, vol. 5897, SPIE, Bellingham, WA, 2005, p. 1, Article CID No. 589702.

[5] Anantaraman, NASA/NSCL SINGLE EVENT EFFECTS TEST FACILITY USER'S MANUAL, National Superconducting Cyclotron Laboratory, Michigan State University, Rev. September 17, 2004.

[6] J.R. Kim, H.M. So, J.W. Park, J.J. Kim, J. Kim, C.J. Lee, S.Ch. Lyu, Appl. Phys. Lett. 80 (2002) 3548.

[7] P. Avouris, Chem. Phys. 281 (2002) 429.

[8] A.B Greytak AB, L.J. Lauhon, M.S. Gudiksen, C.M. Lieber, Appl. Phys. Lett. 84 (2004) 4176.

[9] LabVIEW (National Instruments v7.1).

[10] M.V. O'Bryan, C.M. Seidleck, M.A. Carts, J.W. Howard Jr., H.S. Kim, J. D. Forney, K.A. Label, C.J. Marshall, R.A. Reed, A.B. Sanders, D.K. Hawkins, S.R. Cox, S.P. Buchner, T.R. Oldham, J. Sutton, T.L. Irwin, E. Rodriguez, D. McMorrow, S.D. Kniffin, R.L. Ladbury, M. Walter, C. Palor, P.W. Marshall, M. McCall, S. Meyer, J. Lintz, J. Rodgers, S. Mohammed, D. Rapchun, Rad. Eff. Data Works, July 22, 2004, p. 10.

[11] M. He, P. Zhou, S.N. Mohammad, G.L. Harris, J.B. Halpern, R. Jacobs, W. L. Sarney, L. Salamanca-Riba, J. Cryst. Growth 231 (2001) 257.

[12] M. He, I. Minus, P. Zhou, S.N. Mohammad, J.B. Halpern, R. Jacobs, W.L. Sarney, L. Salamanca-Riba, R.D. Vispute, Appl. Phys. Lett. 77 (2000) 3731.

[13] SRIM: Stopping and Range of Ions in Matter, http://groups.nscl.msu.edu/srim/srim.html.